An Unexpected Role for the Active Site Base in Cofactor Orientation and Flexibility in the Copper Amine Oxidase from *Hansenula polymorpha*†

Julie Plastino,‡ Edward L. Green,§ Joann Sanders-Loehr,§ and Judith P. Klinman*,‡,||

Department of Chemistry, University of California, Berkeley, California 94720, Departments of Chemistry and Molecular and Cell Biology, University of California, Berkeley, California 94720, and Department of Chemistry, Biochemistry and Molecular Biology, Oregon Graduate Institute of Science and Technology, Portland, Oregon 97291

Received November 9, 1998; Revised Manuscript Received March 15, 1999

ABSTRACT: The role of the active site aspartate base in the aminotransferase mechanism of the copper amine oxidase from the yeast *Hansenula polymorpha* has been probed by site-directed mutagenesis. The D319E mutant catalyzes the oxidation of methylamine and phenethylamine, but not that of benzylamine. k_{cat}/K_m for methylamine is found to be 80-fold reduced compared to that of the wild type. Viscosogen and substrate and solvent deuteration have no effect on this parameter for D319E, which is suggestive of limitation of k_{cat}/K_m by a conformational change. This conformational change is proposed to be the movement of the cofactor into a productive orientation upon the binding of substrate. In the absence of substrate, a flipped cofactor orientation is likely, on the basis of resonance Raman evidence that the C5 carbonyl of the cofactor is less solvent accessible than the C3 hydrogen. k_{cat} for D319E methylamine oxidase is reduced 200-fold compared to that of the wild type and is unaffected by substrate deuteration, but displays a substantial solvent isotope effect. A 428 nm absorbance is evident under conditions of saturating methylamine and oxygen with D319E. The D319N mutant is observed to produce a similar absorbance at 430 nm when treated with ammonia despite the fact that this mutant has no amine oxidase activity. Resonance Raman spectroscopy indicates the formation of a covalent ammonia adduct and identifies it as the deprotonated iminoquinone. In contrast, when the D319E mutant is reacted with ammonia, it gives predominantly a 340−350 nm species. This absorbance is ascribed to a localization of the cofactor oxyanion induced by binding of the cation at the active site and not to covalent adduct formation. Resonance Raman spectroscopic examination of the steady state species of D319E methylamine oxidation, in combination with the kinetic data, indicates that the 428 nm species is the deprotonated iminoquinone produced upon reoxidation of the reduced cofactor. A model is proposed in which a central role of the active site base is to position the free cofactor and several enzyme intermediates for optimal activity.

Copper amine oxidases are found in bacteria, fungi, plants, and mammals (*1*) and catalyze the oxidative deamination of primary amines to produce aldehydes, hydrogen peroxide, and ammonia. The presence of these enzymes in prokaryotes and fungi permits the use of substituted amines as a nitrogen source. The function of the copper amine oxidases in higher organisms is uncertain, but is linked primarily to the metabolism of polyamines and biogenic amines (*1*, and references therein). Additionally, an increasingly large body of evidence for hydrogen peroxide as a second messenger in multicellular organisms (*2*) raises the possibility that the copper amine oxidases play an as yet undescribed role in the signaling pathways of higher organisms.

The copper amine oxidases contain a modified tyrosine residue as the active site redox center: 6-hydroxydopa quinone or topa quinone (TPQ)[1] (*3*). Recent studies show that TPQ is produced by the post-translational modification of an active site tyrosine by enzyme-bound copper and oxygen (*4*, *5*). There is strong evidence for an aminotransferase mechanism in the TPQ-containing amine oxidases (see ref *6* for a review). Substrate activation occurs through covalent addition of amine substrate to cofactor, resulting in the labilization of the hydrogen α to the nitrogen. After proton abstraction, the product imine is hydrolyzed to release aldehyde and the cofactor is reoxidized by molecular oxygen. The proton is believed to be abstracted by an active site base, which is suggested by various workers to be a carboxylate (*7*), a histidine (*8*), and a lysine (*9*). Recent crystallographic work (*10*−*12*) has indicated the presence of an active site aspartate, one of 33 absolutely conserved residues in the 11 known amine oxidases ranging in source from bacteria to humans (*10*). Site specific mutagenesis of this aspartate to 12 other residues in the copper amine oxidase from *Escherichia coli* resulted in a complete loss of activity in all but the

† This research was supported by grants from the NIH (GM 39296 to J.P.K. and GM 34468 to J.S.-L.).

* To whom correspondence should be addressed.

‡ Department of Chemistry, University of California.

§ Oregon Graduate Institute of Science and Technology.

|| Departments of Chemistry and Molecular and Cell Biology, University of California, Berkeley.

[1] Abbreviations: TPQ, topaquinone or 6-hydroxydopa quinone; WT, wild type; ECAO, *Escherichia coli* amine oxidase; PSAO, pea seedling amine oxidase; PEAO, *Arthrobacter globiformis* phenethylamine oxidase; HPAO, *Hansenula polymorpha* amine oxidase; ICP, inductively coupled plasma; SDS−PAGE, sodium dodecyl sulfate−polyacrylamide gel electrophoresis; BSAO, bovine serum amine oxidase.

10.1021/bi9826660 CCC: $18.00
Published on Web 06/03/1999

glutamate mutant, which had an activity reduced 10^5-fold compared to that of WT ECAO (*13*).

One of the remarkable features of the TPQ-containing copper amine oxidases is that they perform two related but different reactions: the biogenesis of their own cofactor from a precursor tyrosine and the use of the mature TPQ in catalysis. A major challenge has been to understand the structural basis of this dual functionality. Although the detailed mechanism of cofactor biogenesis has yet to be elucidated, proposed pathways invoke a variety of configurations for the intermediates leading from tyrosine to TPQ (*14*, *15*). In keeping with this requirement for flexibility, alternate cofactor conformations in native copper amine oxidases have been observed in the crystal structures of ECAO, PSAO, and PEAO (*10*, *11*, *13*, *16*). However, this flexibility contrasts with the expectation that the cofactor will remain fixed during the catalytic cycle. Cai et al. have already shown that mutation of the glutamate which flanks the cofactor leads to the accumulation of the product Shiff base intermediate and resulting enzyme inhibition with methylamine as the substrate (*17*). This phenomenon is attributed to a rotation of the cofactor−product imine complex to an inactive conformer as a result of disruption of the interactions which hold the cofactor in place. More recently, Schwartz et al. (*37*) have demonstrated a similar effect upon mutation of the asparagine that flanks the cofactor toward the N-terminus.

In this study, a combination of UV−vis spectroscopy, resonance Raman spectroscopy, and kinetic analysis of site-directed mutants has been used to evaluate the effects of mutation of the active site aspartate, residue 319 in HPAO. Contrary to expectations, it has not been possible to prepare and characterize stable substrate imine complexes of the cofactor. Rather, evidence is provided for altered cofactor conformations which affect the reactivity and the stability of catalytic intermediates and implicate the active site base as an important residue in the maintenance of the cofactor orientation during turnover.

EXPERIMENTAL PROCEDURES

Mutagenesis. Mutagenesis was performed with a Chameleon kit (Stratagene) using an *Aat*II selection system. WT HPAO template and mutants were manipulated in a pDB20 plasmid (*14*). A ca. 50-amino acid stretch surrounding the mutation site was sequenced using a T7 Sequenase kit (U.S. Biochemicals) by the glycol/heat denaturation procedure. *Saccharomyces cerevisiae* strain CG379 was transformed with mutant DNA using the lithium acetate transformation procedure, and transformants were selected for and maintained on uracil drop-out plates, as described for the WT (*14*).

Protein Purification. The mutant protein was purified by the WT HPAO procedure (*14*) with the following modifications. Mutants were grown in Ura^- media supplemented with adenine, histidine, and tryptophan at a concentration of 100 mg/mL each and leucine at a concentration of 150 mg/mL. One hundred milliliters of media was inoculated with cells from a plate and allowed to grow to saturation while it was being shaken at 30 °C. Ten milliliters of this culture was used to inoculate a 250 mL culture which was grown to saturation. Eighteen liters of media (12 × 1.5 L in 4 L flasks) was prepared, and each flask was inoculated with 20 mL of the 250 mL culture. Upon reaching saturation, cells were harvested by centrifugation at 4000*g* for 15 min at 4 °C. The cells were washed once with water and usually frozen at −20 °C, although occasionally lysis was immediately performed. The yield of wet cells was 80−90 g.

The cells were resuspended in 100 mL of 100 mM potassium phosphate buffer (pH 7.0) and lysed by sonication using a Branson Sonifier 450 apparatus fitted with a macrotip. Sonication was performed (in a discontinuous manner to avoid overheating) in a Rosette cell for a total of 4−7 h; the temperature was maintained below 15 °C. The sonicant was centrifuged at 27000*g* for 1 h at 4 °C, and the supernatant was dialyzed against 5 mM potassium phosphate (pH 7.0); no ammonium sulfate precipitation was performed. The dialysate was then centrifuged at 27000*g* for 30−60 min at 4 °C to remove the precipitated material before loading on a Sepaharose CL-6B DEAE (Pharmacia Biotech) anion exchange column, equilibrated in 5 mM potassium phosphate (pH 7.0) at 4 °C. The resin volume of the DEAE column was 500 mL. The protein was eluted as previously described with a linear phosphate gradient: 5 to 100 mM potassium phosphate (pH 7.0) in a total volume of 600 mL.

Fractions were analyzed by SDS−polyacrylamide gels (10%). Fractions containing the 76 kDa band were pooled and concentrated in a 180 mL Amicon concentrator fitted with an XM50 membrane. The protein was loaded onto a Sephacryl S-300 (Pharmacia Biotech) gel filtration column (100 cm long, 1.5 cm inner diameter) equilibrated in 50 mM potassium phosphate (pH 7.0). Fractions were assayed by SDS−PAGE; impure fractions were combined and concentrated using the Amicon apparatus and reloaded on the S-300 column. Pure fractions were pooled and concentrated in a standard collodion apparatus (Schleicher and Schuell) equipped with a 25 kDa molecular mass cutoff collodion membrane. Eighteen liters of culture generally yielded 15−20 mg of protein, as determined by the Bradford protein assay (Bio-Rad). The protein was >95% pure as determined by SDS−PAGE.

General Characterization via TPQ Content, Metal Analysis, and Activity Assay. The estimate of cofactor content by phenylhydrazine titration as previously described for WT HPAO (*14*) could not be routinely performed with the active site base mutants, due to the slowness of the labeling reaction. To allow quantification of TPQ by 480 nm absorbance assessment of the mutants, an estimate of the extinction coefficient for TPQ in D319E was determined. The protein was incubated anaerobically at 37 °C with 3.5 molar equiv of [^{14}C]phenylhydrazine (California Bionuclear, 25 mCi/mmol) in 50 mM potassium phosphate buffer (pH 7.2) for 55 min. Two more additions of 2.5 molar equiv of labeling reagent were made over the next hour to ensure that an end point had been reached. At a total reaction time of 2 h, when the absorbance at 448 nm appeared to have stabilized, the derivatized protein was desalted on a prepacked DG-10 sizing column (Bio-Rad), equilibrated in 50 mM potassium phosphate (pH 7.2), and the protein fractions were pooled. The radioactivity was quantified by liquid scintillation counting using a LKB Wallac instrument, and the protein concentration was determined by the Bradford protein assay, using a molecular mass of 75 731 g/mol of subunit (*5*). The incorporation of radioactive label allowed a calculation of the ratio of TPQ to protein subunit, and a comparison of the

stoichiometry of radiolabeled protein to absorbance at 480 nm led to a calculated extinction coefficient of ca. 1800 M^{-1} cm^{-1} for underivatized cofactor in D319E. Since an end point could not even be approximated with D319N, it was assumed to have an extinction coefficient similar to that of D319E.

The copper content of the active site base mutants was determined by ICP with a five-point standard curve ranging from 0 to 1000 μg/L copper. Protein samples were diluted into deionized water to 100 μg/mL to afford copper readings of approximately 100 μg/L. The limit of detection was 20 μg/L. The copper content was assessed using the 324 nm emission line.

Benzylamine oxidase activity was measured by monitoring the increase in absorbance at 250 nm [$\epsilon = 12.8$ mM^{-1} cm^{-1} (*18*)] due to the product benzaldehyde. The assay was performed in 100 mM potassium phosphate buffer (pH 7.0) at 37 °C with 8.8 mM benzylamine using a Hewlett-Packard 8452-A diode array spectrophotometer. Twenty to seventy micrograms of the protein was used per assay. Methylamine activity was monitored at 37 °C by recording the rate of O_2 consumption using a YSI model 5300 biological oxygen monitor. For D319N, activity was assessed at 3.74 mM methylamine in 100 mM potassium phosphate buffer (pH 7.44), adjusted to an ionic strength of 300 mM with potassium chloride. Up to 134 μg of protein was used per assay. A full investigation of D319E methylamine oxidase activity was performed using the oxygen electrode as follows.

The D319E used for the kinetic characterization was >95% pure as assessed by SDS−PAGE. The protein concentration was determined by the Bradford protein assay, and the cofactor content was estimated as described above. Standard assays at 37 °C and pH 7.44 with 100 mM potassium phosphate, a 300 mM ionic strength, and 2.5 mM methylamine were performed in triplicate at the beginning of each data collection, for use as a frame of reference. The protein exhibited no loss or gain of activity over the course of these studies, and proteins from different preparations were found to have the same turnover number of 0.07 s^{-1} as determined by standard assay.

pH Profiles and Isotope Effects Measurements. Initial velocities for the oxidation of phenethylamine (Sigma), [$^1H_3$]-methylamine, and [$^2H_3$]methylamine (Aldrich) were obtained by monitoring O_2 consumption at 37 °C. Buffers were incubated at 37 °C before being used, and the assay mixture was allowed to equilibrate while it was being stirred for 3 min before the electrode probe was inserted. Twenty to eighty micrograms of enzyme containing ca. 50% TPQ was injected per assay in a volume of 2−5 μL, and rate measurements were taken within the first 5−15% of the reaction. Methylamine activity was measured for both protio and deutero substrates at seven pH values, ranging from 6.55 to 9.76. Phenethylamine activity was measured at three pH values: 7.44, 8.59, and 9.19.

Assays conducted in the pH range of 6.55−7.97 were buffered with 100 mM potassium phosphate, and those in the pH range of 8.59−9.76 were buffered with 25 mM potassium pyrophosphate. All assays were adjusted with potassium chloride to an ionic strength of 300 mM. k_{cat} and k_{cat}/K_m at each pH were obtained by a nonlinear fit to the Michaelis−Menten equation using the program Kaleidagraph. pK_a values were extracted by plotting the log of k_{cat}/K_m versus pH and fitting the resulting curve to a single pK_a with the equation $\log(k_{cat}/K_m) = \log(k_{cat}/K_m)_{max} - \log[1 + 10^{(pK_a - pH)}]$. Errors for p$K_a$ and $(k_{cat}/K_m)_{max}$ values are generated by the fitting program. In cases where means were determined, errors are reported as the standard deviation from the mean.

Solvent Isotope Effects. Initial rates for the oxidation of methylamine by D319E were determined in D_2O using the oxygen electrode as described above. The pH meter electrode was soaked in D_2O before use, and 0.4 was added to the pH readings to give pD values (*19*). Potassium phosphate, potassium bicarbonate, and methylamine were dissolved in D_2O and lyophilized to dryness three times to replace all exchangeable protons with deuterons. Potassium chloride was dissolved in D_2O once and lyophilized to dryness. Anhydrous potassium pyrophosphate and potassium carbonate were placed in a vacuum desiccator for 24 h before use. All buffers and reagents were stored in desiccators, and exposure to atmospheric moisture was minimized during handling and use. The oxygen electrode probe was stored in D_2O between assays.

D319E activity was measured over the pD range of 7.41−7.98 buffered with 100 mM potassium phosphate and 8.42−10.20 buffered with 25 mM potassium pyrophosphate. All assays were maintained at a constant ionic strength of 300 mM with potassium chloride. k_{cat} and k_{cat}/K_m values at each pD were determined, and pK_a values for these parameters were obtained as described above.

Viscosity Studies. Methylamine oxidase activity was monitored at pH 7.97 with 100 mM potassium phosphate and an ionic strength of 300 mM at 37 °C as a function of glucose concentration. The relative viscosities of reaction solutions at 0, 8, 15, 22, 26, and 30 wt % glucose were determined with a viscometer thermostated at 37 °C. The relative viscosities were found to be 1, 1.19, 1.41, 1.72, 1.92, and 2.19, respectively. These numbers were the average of five determinations at each glucose concentration.

Analysis of the Adducts of D319N and Ammonium Ion and D319E and Methylamine by Resonance Raman Spectroscopy. Raman spectra were obtained on a McPherson 2061 spectrograph (0.67 m, 1800-groove grating) using a Kaiser Optical holographic supernotch filter and a Princeton Instruments (LN-1100PB) liquid N_2-cooled CCD detector. The excitation source was a Coherent Innova 90-6 Ar+ laser. Spectra were collected from samples in glass melting point capillary tubes, cooled to ice temperature in a copper coldfinger, using 514.5 nm excitation (30 mW), 90° scattering geometry, and a 4 cm^{-1} spectral resolution. Peak frequencies were calibrated relative to an indene standard and are accurate to ± 1 cm^{-1}. Spectra of samples substituted with isotopes were obtained under identical instrumental conditions such that the frequency shifts were accurate to ± 0.5 cm^{-1} (*20*).

A stock solution of the D319N mutant (1.25 mM in protein monomer, ca. 0.75 mM in TPQ) was prepared in 50 mM potassium pyrophosphate (pH 9.0). The ammonia adduct was formed by the addition of 3 M ammonium chloride which yielded final concentrations of 0.5 M ammonium chloride and 0.6 mM TPQ. Isotopic labeling was performed by the addition of [^{15}N]ammonium chloride (99 at. % ^{15}N, Cambridge Isotope Laboratories) prepared in H_2O or D_2O, as needed. The D_2O sample was prepared by diluting the 1.25 mM protein 10-fold in D_2O buffer (pH reading of 9.0) and

incubating for 22 h at 4 °C before being concentrated back to 1.25 mM by ultrafiltration (Micron-30, Amicon). Data collection times were 15 min.

A stock solution of D319E (1.0 mM in protein monomer, ca. 0.45 mM in TPQ) was prepared in 50 mM potassium phosphate (pH 7.0). The methylamine adduct was formed by the addition of 250 mM methylamine which yielded final concentrations of 42 mM methylamine and 0.38 mM TPQ. To ensure adequate amounts of O_2 for the reaction, the protein and methylamine solutions were flushed with O_2 for 10 min. These solutions were transferred in gastight syringes to a preflushed sample holder, a modified pasteur pipet that was flame-sealed at the capillary end and fitted with a serum stopper on the other end (*20*)**.** Raman spectra were collected immediately after mixing as a series of 1 min scans. Isotopic labeling was performed by the addition of [^{15}N]methylamine (98 at. %, Cambridge Isotope Laboratories) or [$^2H_3$]-methylamine (98 at. %, Aldrich) or by preparation of the protein in D_2O, as described above.

^{18}O Exchange at C5 and D Exchange at C3. For ^{18}O exchange, samples of D319N and D319E (0.75 mM in TPQ) in 50 mM potassium pyrophosphate (pH 7.0) were diluted 14-fold with $H_2{}^{18}O$ (90 at. % ^{18}O) in 50 mM potassium pyrophosphate (pH 7.0), prepared from a 95−98 at. % ^{18}O stock (Cambridge Isotope Laboratories). These solutions were concentrated 17-fold by ultrafiltration and then subjected to a second dilution in $H_2{}^{18}O$, followed by reconcentration to yield 0.75 mM TPQ in 89.6 at. % ^{18}O. Following the 1 h exchange, performed at 6−14 °C, the samples were chilled to 5 °C and 15 min Raman spectra were collected at 2 h intervals using 514.5 nm (50 mW) excitation. The extent of ^{18}O exchange was determined by the intensity of the C5═^{18}O stretch at 1656 cm^{-1} in D319E and at 1652 cm^{-1} in D319N. The ^{18}O-insensitive TPQ mode at 1404 and 1402 cm^{-1}, respectively, was chosen as an internal intensity standard. The reaction appeared to have reached completion by the 26 h time point, and this was assumed to represent 100% exchange. The fraction exchanged, F, was calculated as I_{1650}/I_{1400} at time t divided by I_{1650}/I_{1400} at 26 h. Deuterium exchange measurements were performed after a single 20-fold dilution with D_2O-containing buffer prepared from a 99.9 at. % D stock (Aldrich), followed by reconcentration which yielded 1.5 mM TPQ in 90 at. % D. The extent of D exchange was determined by Raman spectroscopy from the intensity of the C3−D deformation mode at 1299 cm^{-1} in D319E and 1297 cm^{-1} in D319N.

UV−Vis Spectroscopy. Spectral changes of the active site base mutants and WT HPAO in complexes with various amines and other cations were followed at 20 °C using a Hewlett-Packard diode array spectrophotometer. For all data described in Table 3, spectra were collected in 100 mM potassium pyrophosphate buffer (pH 9.0) with 20−40 μM protein subunit (50−60% TPQ). Reagents and approximate concentrations were as follows: 30 mM ammonium chloride (Fisher), 140 mM cesium chloride (Sigma), 30 mM dimethylammonium chloride (Aldrich), and 20−50 mM benzylamine hydrochloride (Sigma). The extent of complexation was calculated from difference spectra using an extinction coefficient of 1800 M^{-1} cm^{-1} for the bleaching of the cofactor at 480 nm for D319E and D319N and an extinction coefficient at 480 nm for WT HPAO of 2400 M^{-1} cm^{-1}. The concentration of the complex was estimated from the observed loss in absorbance at 480 nm, and extinction coefficients for the complexes were estimated from absorbance changes in difference spectra. Spectra shown in Figures 4 and 5 were collected in 50 mM potassium phosphate (pH 7.2); the data for WT HPAO with methylamine were obtained under an oxygen atmosphere, to ensure that the assay was fully saturating in oxygen.

RESULTS

General Comparison of the Active Site Base Mutants to WT. The copper content of D319E and D319N was assayed to be approximately that of WT, one copper per subunit. The cofactor content for preparations of D319N and D319E was assessed by measuring the 480 nm absorbance of the protein at 20−40 mg/mL, using an extinction coefficient of 1800 M^{-1} cm^{-1} for both mutants. The active site mutants produce TPQ at about the same level as WT HPAO, 0.4−0.6 TPQ per protein dimer. Phenylhydrazine determination of TPQ content was not routinely performed due to the low reactivity of the active site base mutants with this inhibitor. The D319E mutant required several hours to reach an end point, and D319N was even less reactive; 1% of the expected absorbance change occurred in 15 min. Phenylhydrazine decomposes over time in the presence of oxygen and/or light, generating radicals which damage protein (*21*). Though not a consideration for WT HPAO where reaction is complete in 20−30 min, the lability of phenylhydrazine posed a problem for the mutants. Our rough estimate of 1800 M^{-1} cm^{-1} for the extinction coefficient at 480 nm for the D319E mutant (see Experimental Procedures) may be compared to an extinction coefficient of ca. 2400 M^{-1} cm^{-1} for the wild type enzyme (*22*) and 2100 M^{-1} cm^{-1} at 498 nm in acetonitrile for TPQ model compounds (*23*). It is possible that the estimated extinction coefficient for the TPQ in D319E and D319N is somewhat low, due to nonspecific labeling of protein with radiolabeled phenylhydrazine during the long incubation times required for the derivatization of TPQ.

D319N was found to have neither methylamine **n**or benzylamine oxidase activity under the given assay conditions. D319E had no detectable benzylamine oxidase activity but was active with both methylamine and phenethylamine. Table 1 briefly compares D319E methylamine and phenethylamine oxidase activity with that of WT. For pH-dependent parameters, the extrapolated maximal values provided by the fitting program were used in the comparison. The k_{cat} for D319E is 200-fold reduced from the extrapolated maximal k_{cat} of WT HPAO with methylamine as a substrate and 80-fold reduced from WT k_{cat}/K_m at the pH maximum for both proteins. In the case of D319E, the k_{cat} for phenethylamine oxidase activity is exactly that of methylamine activity and k_{cat}/K_m is 16-fold higher. For WT HPAO, k_{cat} for phenethylamine is slightly increased over that of methylamine and k_{cat}/K_m is modestly increased. As a result, k_{cat}/K_m for D319E phenethylamine oxidation is reduced from that of WT HPAO only ca. 15-fold and k_{cat} is reduced ca. 240-fold (Table 1). The reduction in k_{cat} for D319E is independent of substrate, while changes in k_{cat}/K_m vary with substrate. As will be described in greater detail, this has important implications for differences in the nature of rate-limiting steps of D319E and WT enzymes.

Table 1: Comparison of the Methylamine and Phenethylamine Activities of D319E and WT HPAO[a]

	k_{cat} (D319E:WT)	k_{cat}/K_m (D319E:WT)
methylamine	1:200[b]	1:80[c]
phenethylamine[d]	1:240	1:15

[a] WT HPAO characterizations were previously carried out at 25 °C (*29*). WT HPAO activity was, therefore, reanalyzed at pH 9.19 and 37 °C, exhibiting a 1.5-fold increase in k_{cat} and a 1.9-fold increase in k_{cat}/K_m relative to the 25 °C data. These corrections were applied to the WT data for comparison to the D319E data at 37 °C. [b] This comparison was made with an extrapolated maximum of 12 s^{-1} for WT at 25 °C. The apparent maximum (ca. 5 s^{-1} at 25 °C) is depressed from the theoretical maximum due to the similarity of the two pK_a values in the k_{cat} plot (*29*). [c] This comparison was made with the extrapolated maximum of 3.15×10^5 M^{-1} s^{-1} for WT at 25 °C (*29*). The apparent maximum is approximately the same because the two pK_a values are ca. 2 pH units apart. [d] A complete pH profile of WT HPAO phenethylamine activity is not available. However, for WT HPAO at pH 7.35, k_{cat} with methylamine is 1.2-fold higher than with phenethylamine and k_{cat}/K_m is 3-fold larger (S. A. Mills and J. P. Klinman, unpublished results). For comparison to D319E, maximal k_{cat} and k_{cat}/K_m for WT phenethylamine oxidation were estimated by adjusting the WT methylamine values by these factors.

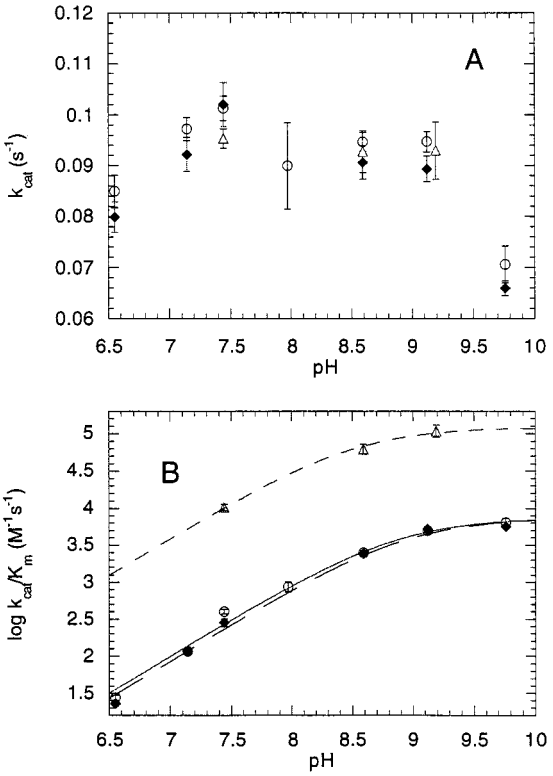

FIGURE 1: pH dependence of k_{cat} and k_{cat}/K_m for D319E with methylamine and phenethylamine: (○) [$^1H_3$]methylamine, (◆) [$^2H_3$]-methylamine, and (△) phenethylamine. (A) For k_{cat}, (○) the mean value = 0.090 ± 0.010 s^{-1}, (◆) the mean value = 0.087 ± 0.012 s^{-1}, and (△) the mean value = 0.094 ± 0.002 s^{-1}. (B) For k_{cat}/K_m, (○) pK_a = 8.87 ± 0.12 and the maximum = (7.4 ± 1.6) × 10^3 M^{-1} s^{-1}, (◆) pK_a = 8.94 ± 0.11 and the maximum = (7.4 ± 1.5) × 10^3 M^{-1} s^{-1}, and (△) the maximum = (1.2 ± 0.2) × 10^5 M^{-1} s^{-1}.

pH Studies and Substrate Isotope Effects with D319E. The pH dependence for k_{cat} using [$^1H_3$]- and [$^2H_3$]methylamine and phenethylamine as substrates is shown in Figure 1A. k_{cat} values for both methylamine and phenethylamine are almost pH-independent. The mean k_{cat} values for [$^1H_3$]- and [$^2H_3$]methylamine oxidation are 0.090 ± 0.010 and 0.087 ± 0.012 s^{-1}, respectively, giving an isotope effect of 1.05 ± 0.19. For phenethylamine, the mean k_{cat} is essentially that of methylamine (0.094 ± 0.002 s^{-1}).

Methylamine enzyme activity may be starting to decrease at higher pH; however, the instability of D319E makes it impossible to confirm this observation. D319E lost 95% of its activity when it was incubated for 8 min at 37 °C in pH 10.0 potassium carbonate buffer. A similar test performed in potassium pyrophosphate (pH 9.8) revealed a moderate decrease in activity. However, intitial rate data could still be collected at this pH, although curvature in the lines was observed. Given this curvature and the error it introduces into the measurement, it is difficult to evaluate the apparent decrease in the k_{cat} profile at high pH. The profile also appears to be decreasing at low pH; however, k_{cat} determined at pH 5.84 (data not shown) is 0.079 ± 0.002 s^{-1}, similar to the value obtained at pH 6.55.

The k_{cat}/K_m pH profiles for the D319E oxidation of methylamine and phenethylamine are shown in Figure 1B. There is no effect of substrate deuteration on k_{cat}/K_m; a maximum k_{cat}/K_m of (7.4 ± 1.6) × 10^3 M^{-1} s^{-1} is obtained for [$^1H_3$]substrate and (7.4 ± 1.5) × 10^3 M^{-1} s^{-1} for [$^2H_3$]-substrate. The values of k_{cat}/K_m are the extrapolated maxima provided by the curve fits and have large errors due to the fact that a true plateau could not be defined because of enzyme instability at high pH. The pK_a values for protio- and deuteromethylamines are 8.87 ± 0.12 and 8.94 ± 0.11, respectively.

The phenethylamine k_{cat}/K_m profile is similar to that of methylamine. However, the extrapolated maximal value for k_{cat}/K_m with phenethylamine is (1.22 ± 0.15) × 10^5 M^{-1} s^{-1}, 16-fold higher than the k_{cat}/K_m for methylamine activity. Additional data in the plateau region at high pH were precluded by the fact that K_m for phenethylamine approached the detection limit. The oxygen electrode does not provide the sensitivity for measuring K_m values below ca. 2 μM at 37 °C.

Solvent Isotope Effects with D319E. The effect of solvent deuteration on the D319E methylamine oxidase steady state parameters k_{cat} and k_{cat}/K_m is shown in overlay plots with the H_2O data in panels A and B of Figure 2, respectively. A pronounced solvent isotope effect on k_{cat} is observed: $^{D_2O}(k_{cat})$ = 2.14 ± 0.31. The pH 9.76 point of the H_2O data is included in the average; the validity of this determination has been discussed above. If the pH 9.76 point is omitted, a mean of 0.094 ± 0.006 is obtained which gives an isotope effect $^{D_2O}(k_{cat})$ of 2.24 ± 0.26. The pK_a in k_{cat}/K_m profiles shifts 0.7 pH unit to a more basic pK_a in D_2O. The direction of this shift is normal for organic acids in D_2O, although the magnitude is somewhat large (*19*). Analogous to the enzyme in H_2O, enzyme denaturation occurred at high pD; at pD 10.53, in potassium carbonate buffer, the enzyme was found to lose its activity too quickly for us to measure initial reaction rates. However, despite the error in the k_{cat}/K_m extrapolated maxima for both D_2O and H_2O, it is apparent that there is little effect of solvent deuteration on the parameter k_{cat}/K_m: $^{D_2O}(k_{cat}/K_m)$ = 1.3 ± 0.4.

Effect of Viscosity on D319E Activity. The effect of viscosogen on the steady state parameters of methylamine activity for D319E is shown in Figure 3. The relative values of k_{cat}°/k_{cat} and $(k_{cat}/K_m)^\circ/(k_{cat}/K_m)$ were plotted versus the relative viscosity η/η°, where the superscript indicates the

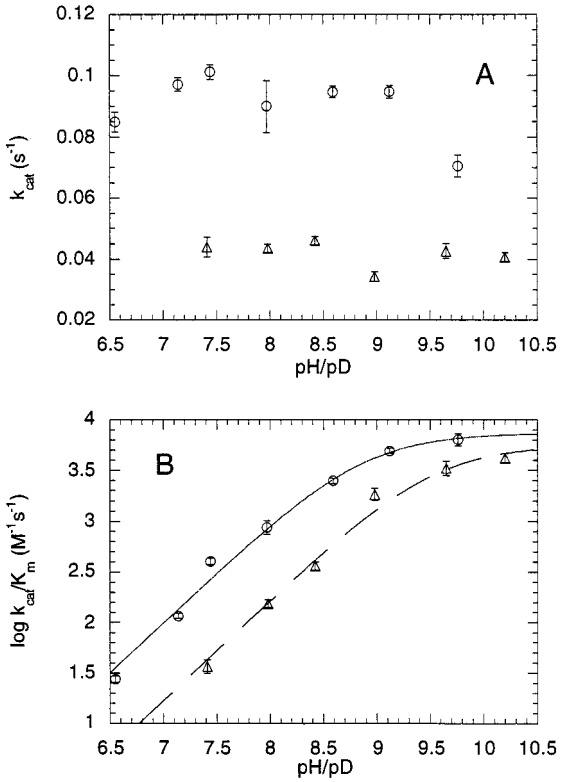

FIGURE 2: Effect of D_2O on k_{cat} and k_{cat}/K_m for D319E with methylamine: (○) H_2O and (△) D_2O. (A) (○) The mean value = 0.090 ± 0.010 s^{-1}; (△) the mean value = 0.042 ± 0.004 s^{-1}, and $^{D_2O}(k_{cat})$ = 2.14 ± 0.31. (B) (○) pK_a = 8.87 ± 0.12, and the maximum = (7.4 ± 1.6) × 10^3 M^{-1} s^{-1}; (△) pK_a = 9.53 ± 0.13, the maximum = (5.7 ± 1.3) × 10^3 M^{-1} s^{-1}, and $^{D_2O}(k_{cat}/K_m)$ = 1.3 ± 0.4.

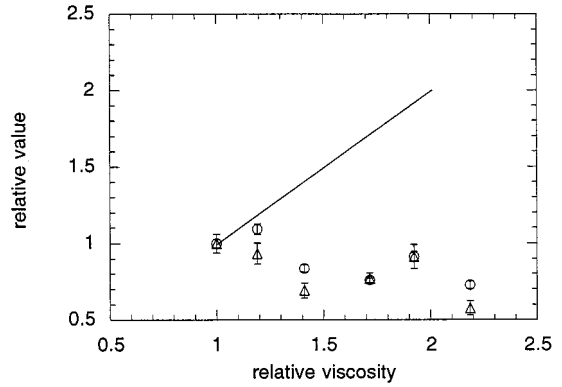

FIGURE 3: Effect of viscosity on the methylamine activity of D319E: (○) $(k_{cat}°/k_{cat})$ and (△) $(k_{cat}/K_m)°/(k_{cat}/K_m)$ with the relative viscosity $\eta/\eta°$. The solid line (slope of 1) represents the theoretical behavior for a fully diffusion-controlled reaction.

absence of the viscosogen glucose. This treatment will give a straight line with a slope of 1 if the reaction is fully viscosity-dependent (shown as a solid line in Figure 3). Slopes of less than 1 indicate varying degrees of viscosity-independent behavior; a slope of 0 indicates that the reaction is not affected by viscosogen (*24*). For $k_{cat}°/k_{cat}$ plots, slopes of less than 0, indicating an increase in activity with added viscosogen, are not unprecedented (*25*, and references therein). The trends in Figure 3 are attributed to a decrease in the concentration of dissolved oxygen with increasing glucose which, when uncorrected, can give small apparent increases in observed rates of oxygen consumption.

Table 2: Rates of Exchange of ^{18}O and D into TPQ of D319E, D319N, and WT HPAO[a]

	D319E	D319N	WT
^{18}O exchange at C5═O	slow	slow	fast
D exchange at C3−H	fast	fast	no[b]

[a] Exchange rates were determined at 5 °C from the increase in Raman spectral intensity at ca. 1655 cm^{-1} for C5═^{18}O and at ca. 1298 cm^{-1} for C3−D. Fast exchange means that the half-time of the reaction is <30 min. Slow exchange means that the half-time of the reaction is 1−4 h. [b] Lack of a deuterium-sensitive peak could be due either to the lack of resonance enhancement of the C3−H deformation or to a complete lack of deuterium exchange.

Figure 3 shows a downward trend in $(k_{cat}/K_m)°/(k_{cat}/K_m)$, as well as $k_{cat}°/k_{cat}$, for D319E and methylamine, indicating that k_{cat}/K_m is not diminished by viscosogen, i.e., that the mutation of the active site base from aspartate to glutamate has not made substrate binding rate-limiting.

Rates of C5═O and C3−H Exchange in Resting Enzymes. Previous studies of the resonance Raman spectra of amine oxidases revealed C═O stretching modes due to the C2 and C5 oxygens of TPQ at 1575 and 1680 cm^{-1}, respectively, as well as a C−H deformation mode of the C3−H at 1310 cm^{-1} (*26*, *27*). These vibrational modes were identified by their substantial downshifts of approximately 25 cm^{-1} upon isotopic substitution with solvent ^{18}O or D and by the corresponding mass spectrum changes in model compounds. The rate of atom exchange at the C5 and C3 postitions, as determined by the change in Raman intensity, appears to correlate with the observed orientation of the TPQ cofactor in the crystal structures of amine oxidases. Thus, HPAO has a productive TPQ conformation with the C5═O oriented toward the catalytic base (*12*), and it exhibits rapid exchange ($t_{1/2}$ < 30 min) of the C5 carbonyl (Table 2). In contrast, PSAO has a flipped TPQ conformation with the C5═O oriented away from the catalytic base (*11*), and it exhibits a much slower rate of exchange ($t_{1/2}$ > 4 h) of the C5 carbonyl (*28*). The D319E and D319N mutants behave like PSAO in that they have slow rates of ^{18}O exchange at the C5 carbonyl and, in addition, they exhibit rapid incorporation of D at the C3 position. This pattern is opposite of that observed with the WT enzyme and indicates an altered environment for the resting cofactor in D319E and D319N; this interpretation is confirmed by kinetic data for D319E, as will be discussed below. The slow rate of ^{18}O exchange with the mutants implies poor accessibilty of the C5 carbonyl to water in this new orientation, and the rapid exchange of deuterium into the C3 ring position indicates enhanced exposure to solvent on the opposite side of TPQ, perhaps as a consequence of a flipped conformation.

UV−Vis Study of the Accumulation of Enzyme Intermediates with the Active Site Base Mutants. Methylamine is turned over by WT HPAO and D319E, but not by D319N. A 428 nm band is the main absorption observed when D319E is incubated with methylamine under conditions of saturating substrate and O_2 at both pH 7.2 (Figure 4) and pH 9.0. This absorbance is also seen with ethylamine and phenethylamine, and peak formation is completely reversible. Under conditions of saturating methylamine and oxygen at pH 7.2 (Figure 5), WT HPAO displays a 308 nm absorbance, characteristic of the reduced cofactor, aminoquinol; similar features are observed at pH 9.0. This is in agreement with the kinetic

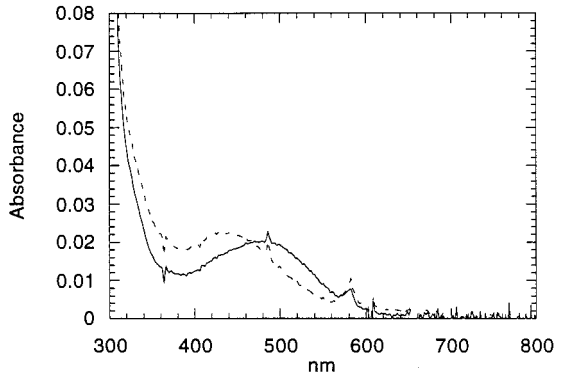

FIGURE 4: Reaction of D319E with methylamine: (—) D319E alone and (- - -) D319E and methylamine. The conditions were 18 μM D319E, 12 mM methylamine, 50 mM potassium phosphate, pH 7.2, and 20 °C.

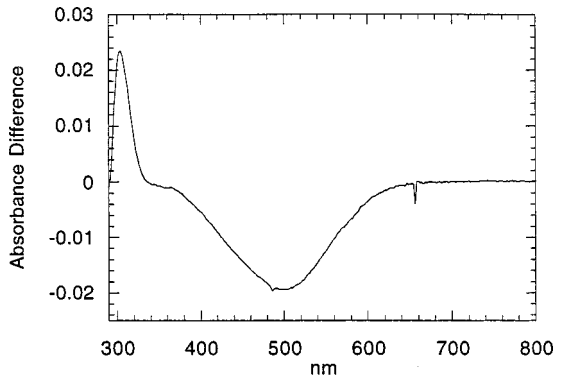

FIGURE 5: Difference spectrum of WT HPAO and methylamine. The difference spectrum was generated by subtracting the spectrum of WT HPAO from the spectrum of WT HPAO with methylamine. The conditions were 6 μM WT HPAO, 0.98 mM methylamine, saturating oxygen, 50 mM potassium phosphate, pH 7.2, and 20 °C.

characterization of this enzyme (*29*) and that of BSAO (*30*) which indicates that the reoxidation of aminoquinol at least partly limits the parameter k_{cat}. When D319N is treated with methylamine at pH 7.2, no spectral changes are produced. At pH 9.0 (data not shown), D319N gives a complex and unexplained spectral pattern when reacted with methylamine, ethylamine, and phenethylamine. The main features are a pronounced absorbance increase at 302 nm and a broadening of the TPQ absorbance. The 302 nm band observed with D319N and methylamine was found to have an extinction coefficient that is at least 6-fold higher than that of the reduced cofactor, and peak formation was completely reversible. These properties, along with the inability to detect any catalytic activity with D319N, eliminate the possibility that the 302 nm absorbance is reduced cofactor.

It was observed that the methylamine spectrum of D319E most closely resembles the adduct formed by ammonium ion treatment of D319N. D319N with ammonium chloride at pH 9.0 gives predominantly a 430 nm species. A similar but much weaker response is observed at pH 7.2. Examination of ammonium ion complexes of WT HPAO and D319E reveals a very different pattern of absorbance changes. WT HPAO and D319E complexes with ammonium chloride afford predominantly a 340−346 nm species at both pH 9.0 and 7.2.

To distinguish absorbance shifts caused by adduct formation from shifts caused by ionic interactions with the cofactor, the effects of cesium ion and dimethylammonium ion were examined; these reagents are not capable of Schiff base formation with TPQ. This later study was prompted by results obtained with methylamine dehydrogenase, where cation shifts of absorbance maxima were mistakenly assigned to ammonia adduct formation (*31*, and references therein). Table 3 summarizes the λ_{max} values of the major absorption bands for the various complexes and the approximate extinction coefficients (see Experimental Procedures for this calculation). The peak frequencies in the difference spectra reported in Table 3 are reproducible, but the extinction coefficients are variable (±50%) depending on the quality of the difference spectra. Extinction coefficients have been included so that trends in peak magnitudes can be compared.

Table 3: Main Absorbance Features for WT, D319E, and D319N upon Treatment with Ammonium, Cesium, and Dimethylammonium Ions and with Benzylamine[a]

		WT	D319E	D319N
1	NH_4Cl	340 nm (5300)	346 nm (3400)	430 nm (1300)
2	cations			
	CsCl	346 nm (nd[b])	346 nm (5500)	no reaction
	$(CH_3)_2NH_2Cl$	346 nm (4500)	346 nm (2300)	no reaction
3	benzylamine	nd[b]	350 nm (6700)	no reaction

[a] All data were collected at pH 9.0. Minor spectral features have been omitted. Approximate extinction coefficients in M^{-1} cm^{-1} are indicated in parentheses beneath each absorbance and represent lower limits as they are based on the assumption that all of the TPQ is converted to the major complex. [b] Not determined.

The results of reaction of WT HPAO, D319E, and D319N with ammonium chloride are summarized in Table 3 (entry 1). Spectral changes produced by cesium chloride and dimethylammonium chloride at pH 9.0 are summarized in Table 3 (entry 2). Both WT HPAO and D319E give a 346 nm absorbing species with cesium chloride at pH 9.0, and D319N is unaffected by cesium chloride treatment. Dimethylammonium chloride produces predominantly a 346 nm species with WT HPAO and D319E. D319E was tested with cesium chloride and dimethylammonium chloride at pH 7.2; absorbance shifts similar to those seen at pH 9.0 were observed, but the extent of complexation was poor. The spectrum of D319N is unaffected by the addition of dimethylammonium chloride. Entry 3 of Table 3 summarizes the behavior of D319E with benzylamine; D319E has no detectable benzylamine oxidase activity. WT HPAO was not studied, and D319N did not react with benzylamine at either pH 9.0 or 7.2. D319E and benzylamine give mainly a 350 nm band. This complex is similar to what is seen with D319E and the cations described in entry 2.

In summary, the λ_{max} and extinction coefficients for the ammonium complexes of D319E and WT HPAO and the benzylamine complex of D319E are similar to those observed for the cesium and dimethylammonium ion complexes. Since these latter reagents are incapable of covalent addition to TPQ, this suggests that the ca. 350 nm absorbances observed with D319E and WT are caused by noncovalent interactions with the cofactor. The only systems which appear to exhibit covalent adduct formation are those which produce the ca. 430 nm species, the steady state species seen during D319E turnover of methylamine and the ammonium complex of D319N. The nature of these species was further investigated by resonance Raman spectroscopy.

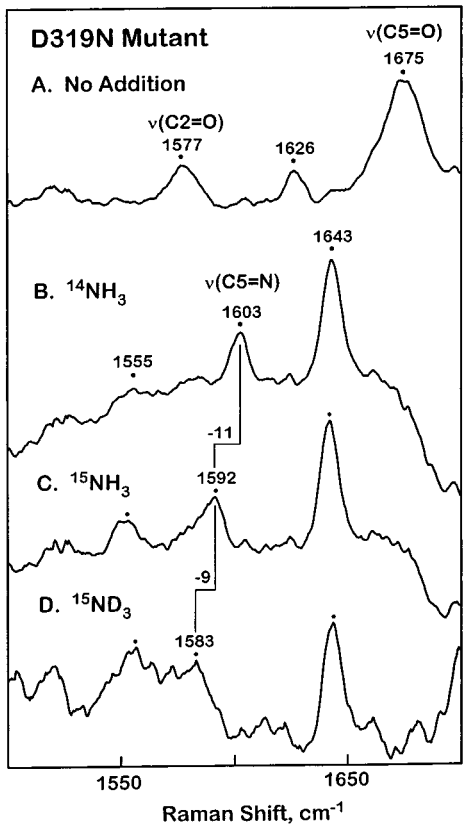

FIGURE 6: Resonance Raman spectra of the ammonia adduct of D319N. Samples were prepared with (B) $^{14}NH_4Cl$ in H_2O, (C) $^{15}NH_4Cl$ in H_2O, (D) and $^{15}NH_4Cl$ in D2O. (A) Sample with no added NH_4Cl. Data were obtained using 15 min data accumulations, and spectra were corrected for water and protein bands by subtraction of the apoprotein spectrum. Frequency shifts relative to spectrum A are indicated above peaks, and peaks with frequencies identical to those of spectrum A are unlabeled.

Resonance Raman Spectroscopy of the Ammonia Adduct of D319N and the Methylamine Adduct of D319E. Resonance Raman spectroscopy of the complexes absorbing at ca. 430 nm was undertaken to determine if the ammonium ion complex of D319N and the major species formed with D319E during methylamine turnover were covalent adducts of TPQ. The ammonium complex of D319N offered a simplified system since the only possible adducts were the carbinolamine and the iminoquinone. As shown in Figure 6, the C5 carbonyl stretch of TPQ at 1675 cm^{-1} is no longer present in the ammonia adduct of D319N. Instead, two new peaks are apparent at 1643 and 1603 cm^{-1}. A 1603 cm^{-1} peak was previously identified as the substrate imine C═N stretch in the aniline adduct of PEAO (*26*). Replacement of [^{14}N]ammonium chloride with [^{15}N]ammonium chloride in the D319N adduct leads to a shift of −11 cm^{-1} for the imine species. This is the expected shift for a change of 1 mass unit given that the change of 2 mass units in the substitution of ^{18}O for ^{16}O at C5 produces a shift of ca. −25 cm^{-1}. Solvent D_2O had little effect on the [^{14}N]ammonia adduct, but shifted the imine stretch a further −9 cm^{-1} in the [^{15}N]-ammonia adduct. This is most consistent with a change of 1 mass unit, indicating the presence of one deuterium on the imine nitrogen. These data suggest that the ammonia adduct of D319N is the deprotonated iminoquinone.

The resonance Raman study of the complex of D319E with methylamine was complicated by the fact that D319E turns over methylamine. Since diffusion of oxygen into the capillary was poor, the oxygen in the sample was rapidly depleted and the steady state 430 nm species was replaced by the reduced cofactor. The data shown in Table 4 indicate the initial formation of a species highly analogous to the ammonia adduct of D319N, with a small peak at 1607 cm^{-1} and a larger peak at 1648 cm^{-1}. The differences in frequency between the D319E and D319N data may indicate slightly different environments in the two enzymes. The 1607 cm^{-1} peak of the D319E methylamine adduct shifts −12 cm^{-1} with [^{15}N]methylamine, similar to the shift observed with [^{15}N]-ammonium chloride and D319N. The 1607 cm^{-1} peak does not shift to lower energy in D_2O; however, we note that while there is a shift of −9 cm^{-1} with D_2O for the [^{15}N]-methylamine complex of D319N, there is no effect of D_2O on the [^{14}N]methylamine sample. This could mean that the C═^{14}N is more coupled to other modes than the C═^{15}N stretch. No shifts are apparent upon formation of the adduct with [$^{2}H_3$]methylamine, which indicates that the methyl group of the substrate is no longer present in the methylamine adduct of D319E. This helps to rule out the possibility that the 430 nm species is the substrate Schiff base, although the signal to noise in this experiment is such that a small shift upon isotopic substitution could have gone undetected. However, the similarity of the resonance Raman data for the methylamine adduct of D319E and the ammonia adduct of D319N strongly suggests that the species accumulating during methylamine turnover by D319E is the deprotonated iminoquinone.

Table 4: Raman Frequencies of Iminoquinone Modes in the Ammonia Adduct of D319N and the Methylamine Adduct of D319E[a]

	D319N and ammonia		D319E and methylamine	
mode	fundamental	shift	fundamental	shift
C5═N stretch				
^{15}N	1603	−11	1607	−12
D_2O		−1		0
^{15}N and D_2O		−20		nd[b]
CD_3		na[c]		0
ring	1643		1648	

[a] Frequencies and isotope downshifts upon substitution with heavier mass are reported in cm^{-1}. [b] Not determined. [c] Not applicable.

DISCUSSION

Does the Substrate Schiff Base Accumulate with the Active Site Base Mutants? The catalytic cycle of WT HPAO is shown in Scheme 1 in the unboxed areas. The intermediacy of a substrate Schiff base species has been implicated by chemical trapping experiments using both pro- and eukaryotic copper amine oxidases (*32*, *33*). Additionally, rapid-scanning stopped-flow spectroscopy of benzylamine oxidation by BSAO (*34*) revealed a transient at 340 nm which was assigned to the substrate Schiff base species. This was supported by model chemistry studies which indicated that when the oxyanion of substrate Schiff base compounds was localized either by hydrogen bonding with the protonated imine nitrogen or by an intimate ion pair interaction, absorbance maxima were 340−350 nm; a 454 nm band was seen for a deprotonated substrate Schiff base model compound (*35*). Although product Schiff base complexes of HPAO (*17*), PEAO, and BSAO (*26*) have been shown to

Scheme 1: Proposed Reaction Mechanism for Amine Oxidation by WT HPAO and D319E[a]

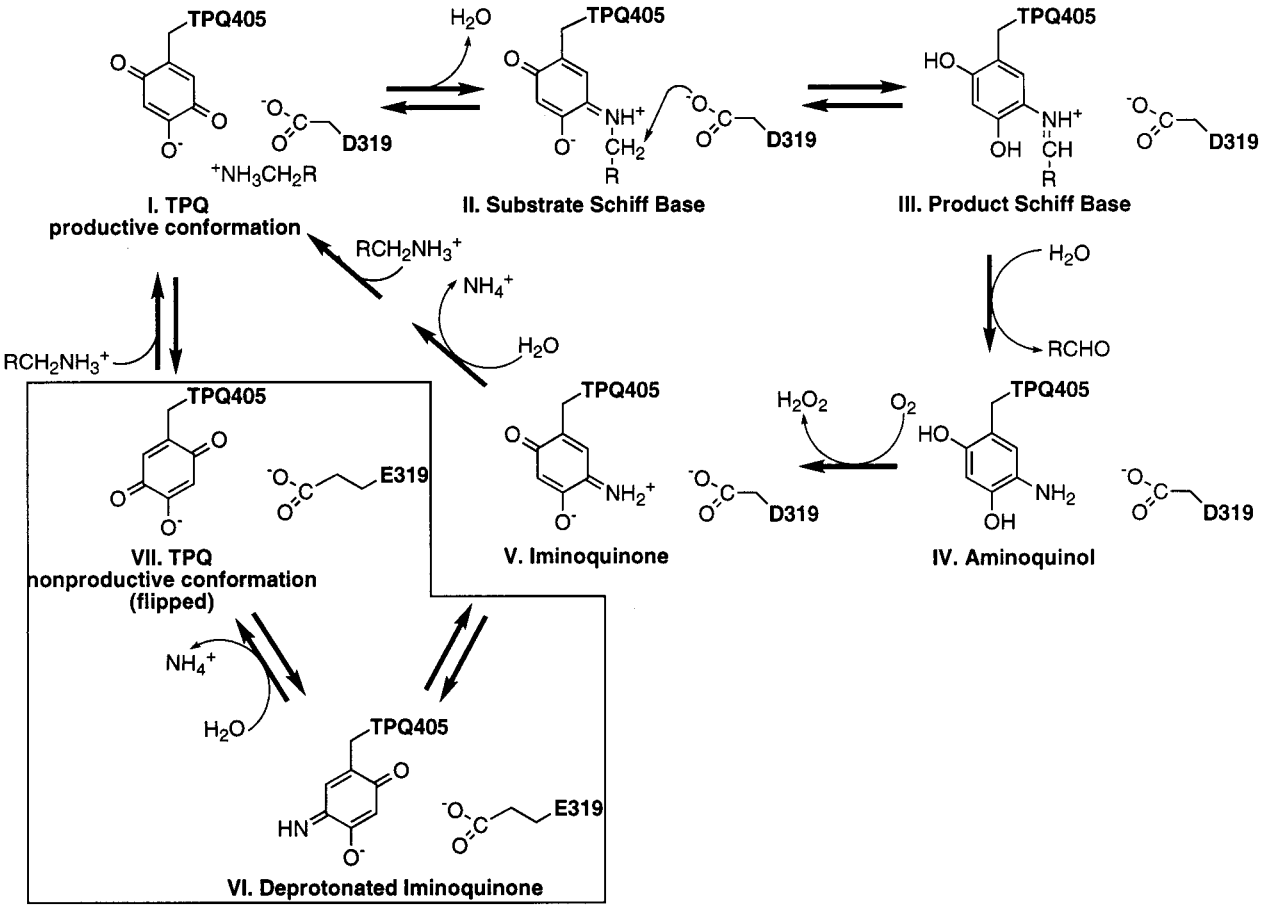

[a] Intermediates pertaining exclusively to the mechanism of D319E are boxed, and the active site base is drawn as a glutamate for these processes. In the WT mechanism, aspartate acts as the active site base to deprotonate substrate and transfer this proton to the 0−4 position of the cofactor (*43*).

accumulate in active site mutants (HPAO) or by the use of unnatural substrates (PEAO and BSAO), establishing conditions for the buildup of substrate Schiff base complexes has not proven to be so tractable. An X-ray crystallographic study of an ECAO−2-hydrazinopyridine complex provided the first direct observation of a substrate Schiff base-like species at an enzyme active site (*13*). A resonance Raman study of a PEAO−aniline adduct (*26*) identified a similar complex. However, both of these characterizations were performed with compounds that are not turned over by the amine oxidases. This makes it difficult to draw inferences regarding the properties of an actual substrate adduct.

One of the motivations behind the generation of active site base mutants of HPAO was the desire to stabilize and characterize the substrate Schiff base complex. However, UV−vis analysis of D319N provides no evidence for accumulation of a substrate Schiff base intermediate. The only adduct formed with D319N is a 430 nm species produced by reaction with ammonium ion. This complex is identified by resonance Raman spectroscopy as the deprotonated iminoquinone formed by addition of ammonia to the C5 carbonyl. An adduct of PEAO and aniline has a similar absorbance and was shown by resonance Raman spectroscopy to be a deprotonated substrate Schiff base type species (*26*). Furthermore, the reaction of BSAO and ammonia at pH 9.13 produced a 450 nm absorbance (*36*), and 448−450 nm absorbances have been observed for iminoquinone model compounds (*35*, *36*).

Under steady state conditions with methylamine, D319E is found to accumulate a 428 nm-absorbing species, similar to the ammonia adduct of D319N, as determined by both UV−vis and resonance Raman spectroscopic analysis. The assignment of the 428 nm absorbance to the iminoquinone rather than to the substrate Schiff base is further supported by the absence of a shift with [$^2H_3$]methylamine in the resonance Raman spectrum and by kinetic analysis of D319E, both of which will be discussed below. Confirmation of the iminoquinone structure at the D319E active site was attempted by reacting D319E with ammonium ion. However, this treatment gives predominantly a 350 nm species. Cations incapable of covalent addition to TPQ, such as cesium ion and dimethylammonium ion, afford 340−350 nm species as well with extinction coefficients similar to that of the D319E ammonium adduct. This strongly suggests that the 340−350 nm absorbance does not arise from covalent addition of the ammonia to the cofactor of D319E, but is produced by binding of a positively charged species in the vicinity of the TPQ and active site base. It is proposed that cesium ion, dimethylammonium ion, and ammonium ion interact with the oxyanion at the C4 position of TPQ, localizing the charge and producing a 340−350 nm species. As documented earlier, the delocalization of the C4 oxyanion through the C2 carbonyl is thought to produce the 498 nm absorbance characteristic of TPQ (*23*). In addition, it was found that the 498 nm absorbance (ϵ = 2100 M^{-1} cm^{-1} in acetonitrile) shifted to 372 nm (ϵ = 700 M^{-1} cm^{-1} in acetonitrile) upon

protonation. A 350 nm band is also observed in the reaction of D319E with benzylamine. However, the extinction coefficient for the D319E−benzylamine complex at 350 nm (ca. 6700 M^{-1} cm^{-1}) is much larger than that obtained for the cyclohexylamine substrate Schiff base model complex absorbance at 352 nm (1300 M^{-1} cm^{-1}) (*35*), which does not support a substrate Schiff base assignment and suggests instead a charge-localized form of cofactor similar to that seen with cesium ion, dimethylammonium ion, and ammonium ion.

The fact that the 340−350 nm species forms most readily at pH 9.0 suggests that the ionization of other active site residues, in addition to the C4 oxygen of cofactor, is necessary for cation binding. A possible candidate is the active site base, aspartate 319 for WT HPAO and glutamate 319 for D319E. The fact that D319N does not form a 340−350 nm species with any reagent at high or neutral pH further implicates an acidic residue at position 319 for binding of cations near the C4 oxyanion of TPQ.

Characterization of D319E. A full kinetic characterization of the methylamine oxidase activity of D319E was undertaken in an effort to describe the mechanistic changes produced by the aspartate to glutamate substitution and to provide further support for the hypothesis that the deprotonated iminoquinone was accumulating during methylamine turnover by D319E.

There are no substrate isotope effects on either k_{cat} or k_{cat}/K_m for D319E, eliminating proton abstraction from substrate as a partially rate-limiting step with either parameter. Although WT HPAO exhibits no isotope effect on k_{cat} for methylamine oxidation, an effect of 4 is seen with k_{cat}/K_m (*29*), interpreted as partial rate limitation by C−H bond cleavage for k_{cat}/K_m and rate limitation of k_{cat} by another process occurring after the irreversible oxidation of substrate in the reductive half-reaction. D319E is the only mutant of HPAO at present which has been shown to be insensitive to substrate methylamine deuteration in both k_{cat} and k_{cat}/K_m.

Unlike WT HPAO methylamine activity, the k_{cat} of D319E exhibits no pH dependence. k_{cat}/K_m however exhibits a curve similar to that seen with WT HPAO with an acidic pK_a of 8.87 ± 0.12. As discussed in the Results, a basic pK_a could not be obtained for D319E due to protein denaturation at high pH. The WT HPAO k_{cat}/K_m curve has an acidic pK_a of 8.00 ± 0.08 and a basic pK_a of 10.13 ± 0.26, which are attributed to the active site base in free enzyme and the free substrate amine, respectively (*29*). A possible explanation for the elevated pK_a of 8.00 for a carboxylate is the proximity of the oxyanion of the cofactor. With a pK_a of 4.13 in model compounds and 3.0 in BSAO (*36*), the C4 oxygen of the cofactor is deprotonated and negatively charged at physiological pH. This active site environment would enhance the basicity of the active site aspartate.

The pK_a of k_{cat}/K_m is further inflated to a value of 8.87 ± 0.12 by the mutation of the active site aspartate to glutamate. Interestingly, D319E is the only active site mutant of HPAO thus far characterized (*29, 37*) that has an altered pK_a in k_{cat}/K_m. In the absence of a substrate isotope effect, it is impossible to assess whether the pK_a in k_{cat}/K_m for D319E is a microscopic or kinetic pK_a. If it is assumed that 8.87 is the pK_a of the active site base in the mutant, the elevation of this value from that of WT may be rationalized by the extension of the side chain which brings the carboxylate closer to the cofactor oxyanion.

Since substrate isotope effects indicate that proton abstraction is not responsible for the large reduction in k_{cat}/K_m and k_{cat} for D319E, viscosity effects and solvent isotope effects were measured for D319E methylamine activity to evaluate the extent of rate limitation by substrate binding (viscosity effects) and the participation of solvent D_2O or solvent-exchangeable protons in the rate-limiting step (solvent isotope effects). Microviscosogens such as glucose inhibit the movement of small molecules in solution. If substrate binding is impaired for D319E because the active site base plays a role in this process, then k_{cat}/K_m should be reduced by the addition of glucose to assay mixtures. The viscosity data do not show a decrease expected for limitation of this parameter by the binding of substrate. Solvent isotope effects are useful in identifying rate-limiting proton transfer steps, although the presence of a solvent isotope effect does not preclude a rate-limiting conformational change. Reorganization of solvent deuterium upon structural change has been seen to give large solvent isotope effects (for two recent examples of this effect, see refs *38* and *39*). For D319E, there is a negligible solvent isotope effect on k_{cat}/K_m, 1.3 ± 0.4, implying that proton transfer steps preceding the formation of the substrate Schiff base or those associated with the hydrolysis of the product Schiff base are not rate-limiting.

The remaining explanations for the k_{cat}/K_m data of D319E invoke either a conformational change of the protein or a realignment of the cofactor. The latter could be movement of the cofactor into an orientation that places the C5 carbonyl in position for attack by amine substrate. The resonance Raman exchange data provide support for this proposal. As shown in Table 2, ^{18}O exchanges more slowly into the C5 position of the cofactor in D319E than in WT HPAO and deuterium exchanges more rapidly into the C3 position in the mutant, implying an altered cofactor environment in the mutant. It is possible that TPQ is in a flipped conformation with the C5 carbonyl pointed away from the substrate channel and therefore less accessible to water, depicted as **VII** in Scheme 1. A flipped conformation for the cofactor was found to be the best fit to the electron density in the ECAO crystal structure, although disorder in the density suggested multiple orientations (*13*). The intact crystals were assayed and shown to be active (*10*). In the PSAO crystal structure, the cofactor was exclusively in the flipped conformation (*11*). The activity of these crystals is not mentioned, though they are reported to be pink (*40*). When these observations with enzymes from other sources are considered, it is possible that D319E may likewise have a flipped cofactor in its resting state. From its fast rate of ^{18}O exchange, an altered conformation for the active site is not expected to be a consideration for WT HPAO. This is consistent with the evidence for partial rate limitation of k_{cat}/K_m by proton abstraction. The crystal structure of WT HPAO shows the cofactor to be properly oriented in the active site with the C5 carbonyl bridged to the active site aspartate through a conserved H_2O molecule (*12*). This interaction may serve to fix the cofactor in the WT HPAO protein. When the aspartate is mutated to a glutamate, the hydrogen bonding network holding the cofactor in place is expected to be compromised, allowing the cofactor to slip into a less accessible conformation in the resting form of D319E. The

binding of the substrate is proposed to induce a ring reorientation which brings the C5 carbonyl of the cofactor close to the active site base and the presumed site of substrate entry into the active site. The lack of substrate and solvent isotope effects on k_{cat}/K_m for D319E points toward rate limitation of this parameter by cofactor reorientation, and the participation of substrate in this process is assumed to be the origin of the large difference in k_{cat}/K_m values for methylamine and phenethylamine.

k_{cat} for the oxidation of methylamine by D319E indicates a sizable solvent isotope effect of 2.14 ± 0.31. As previously discussed, the solvent isotope effect on k_{cat}/K_m is essentially unity. The fact that there are different solvent isotope effects on k_{cat} and k_{cat}/K_m indicates that k_{cat} and k_{cat}/K_m are limited by different processes, with the unique step limiting k_{cat} occurring after the first irreversible step of the reductive half-reaction. The latter is considered to be proton abstraction or, most conservatively, the release of aldehyde. The magnitude of the solvent isotope effect suggests a hydrolytic process, although a conformational change with extensive hydrogen bond rearrangement cannot be eliminated.

The possibility that k_{cat} for D319E must be largely limited by processes after the first irreversible step supports the conclusion from UV−vis and resonance Raman analysis that the 428 nm band observed with D319E and methylamine is the deprotonated iminoquinone and not the substrate Schiff base. This proposal is consistent with the fact that k_{cat} values are virtually identical using either methylamine or phenethylamine as the substrate, a further indication that a step after the release of the aldehyde product is the rate-limiting step in turnover of amines by D319E.

An iminoquinone model compound of TPQ has been reported to hydrolyze slowly at pH 9.0 (*36*). A study with the monoimine of *p*-benzoquinone, which is similar to the iminoquinone of TPQ, but lacks the hydroxyl group ortho to the imine moiety, gave a rate of 0.2 s^{-1} for hydrolysis of the protonated imine and a rate of 10^{-4} s^{-1} for hydrolysis of the deprotonated form, with a reported pK_a of 3.7 for the imine nitrogen (*41*). In WT HPAO, the active site base may interact electrostatically with the iminoquinone to maintain it in the correct orientation and protonation state at physiological pH for rapid hydrolysis; the base may also catalyze the hydrolysis directly. Incorporating what we know about the flexibility of the underivatized cofactor in D319E (cf. the analysis of the k_{cat}/K_m of D319E discussed above), we propose that the accumulation of the iminoquinone with D319E during turnover results from the rapid movement of this intermediate into an altered conformation (possibly flipped) which is less accessible to hydrolysis. Deprotonation, as indicated from resonance Raman studies, occurs as a consequence of cofactor rotation away from the active site base counterion and its removal from the environment of the substrate binding site. In this model, hydrolysis of the deprotonated iminoquinone in the flipped orientation (**VI** in Scheme 1) limits k_{cat}, accounting for the large solvent isotope effect on this parameter and for the fact that the k_{cat} values for methylamine and phenethylamine oxidation are identical. Alternatively, the solvent isotope effect may arise from a proton transfer which is concomitant with the rate-limiting rotation of the iminoquinone back into the productive orientation where rapid hydrolysis occurs. The latter process would be expected to display a pH dependence. While k_{cat} appears to be essentially pH-independent, its pK_a may be shifted out of the observable range.

Mutation of the aspartate at position 319 to asparagine also appears to disrupt the hydrogen bonding network that normally holds the cofactor in a productive conformation. Thus, Raman data for resting D319N show slow exchange of the C5 carbonyl in the $H_2{}^{18}O$ and rapid exchange of the C3 hydrogen in D_2O (Table 2). The ammonia adduct of D319N exhibits similarly rapid exchange of its C3 hydrogen in D_2O, suggesting that the C3 position is on the exposed, catalytic base side of the cofactor. The Raman spectrum of the ammonia adduct of D319N reveals a deprotonated imine. These findings provide further support for the flipped iminoquinone orientation in D319E (**VI** in Scheme 1).

One question that arises from this study is why altered conformations of the substrate and product Schiff base complexes of D319E do not appear to accumulate during turnover. In the case of the active site mutant E406N, the smallest substrate, methylamine, was found to produce mechanism-based inactivation as a result of rotation and deprotonation of the product Schiff base (*17*). The steric bulk of the substrate moiety was thought to prevent ring movement in the product Schiff base complexes of the larger substrates and in the nonplanar substrate Schiff base species. In the case of D319E, steric interactions between the glutamate side chain and both substrate and product Schiff base complexes may serve to maintain both of these species in their productive orientations; however, once the alkyl chain is removed, the cofactor can assume altered conformations in the active site. One might expect cofactor flexibility to also affect the reoxidation of aminoquinol to iminoquinone in D139E. This would potentially be revealed in the parameter k_{cat}/K_m for oxygen, which, unfortunately, could not be obtained due to immeasurably small K_m values for oxygen for D319E.

Concluding Remarks. In comparing the activity of the D319E mutant of HPAO to that of WT, we conclude that alterations in the cofactor configuration in D319E lead to rate-limiting steps under turnover conditions that are completely different from those of the WT enzyme. The outcome of the analysis of the active site base mutants is that, in addition to catalysis of proton abstraction from substrate, a primary role of the aspartate is to maintain the resting cofactor in a reactive conformation. An interesting corollary of this phenomenon is the accumulation of the deprotonated iminoquinone intermediate during D319E methylamine oxidation. We propose that this species is able to rotate in the active site, much like underivatized TPQ, to give an intermediate that is resistant to hydrolysis. These conclusions have been incorporated into the catalytic cycle representation depicted in Scheme 1. The mechanism of D319E is the same as that of WT except for alterations in the structure of the underivatized TPQ and the iminoquinone intermediate, as designated by the boxed areas in Scheme 1.

The crystal structure of WT HPAO shows the cofactor to be in a catalytically productive conformation, hydrogen bonded to a network of water molecules which connects the region of the active site that contains the active site base and catalyzes substrate oxidation to the region that contains

[2] N. K. Williams and J. P. Klinman, unpublished results.

copper ion and catalyzes the reduction of dioxygen to hydrogen peroxide (*12*). This structure raises the possibility that any active site mutations that disrupt the hydrogen bond network could dislodge the cofactor from its optimal configuration for catalysis. This hypothesis is supported by several recent studies where a mutation at the 404, 406, or 305 position in the active site leads to the accumulation of catalytic intermediates in a conformation and/or protonation state that is off the reaction path (*17*, *29*, *37*). Furthermore, in the case of the position 404 mutant, evidence is presented that the resting cofactor is in a nonproductive conformation, similar to the phenomenon observed with D319E and D319N.

It is interesting to note that the rate of biogenesis of TPQ is also affected by the mutation of the active site aspartate to glutamate; the rate of TPQ production in D319E is ca. 90-fold reduced compared to that of WT HPAO.[2] This indicates a possible role for the aspartate in the maintenance of the ring orientation in TPQ precursors as has been shown in this work for the mature TPQ and associated catalytic intermediates. The impact of other active site mutations on TPQ biogenesis is addressed in refs *29*, *37*, and *42*.

NOTE ADDED IN PROOF

The following paper addresses crystal structures for *E. coli* copper amine oxidase that has been mutated at the active site base with Ala, Asn, and Glu (*44*). Although detailed kinetic studies have not been pursued by Murray et al., their overall trends in rate are similar to those reported herein. Their mechanistic conclusions are, however, different regarding the role of cofactor mobility in catalysis. Murray et al. propose that mutants impede cofactor mobility, while we show that mutations at the active site base increase mobility and lead to the accumulation of inhibitory intermediates. This conclusion of increased cofactor mobility in mutant forms of the enzyme is completely consistent with conclusions reached from earlier studies of proteins that had been mutated at residues in the consensus sequence that surrounds the active site cofactor (*17*, *37*). Possible explanations for the differences seen in the two papers may relate to effects of crystal packing or to differences in the pK_a of the active site base in relation to the pH of the study.

REFERENCES

1. McIntire, W. S., and Hartman, C. (1993) in *Principles and Applications of Quinoproteins* (Davidson, V. L., Ed.) pp 97−171, Marcel Dekker, Inc., New York.
2. Sundaresan, M., Yu, Z.-x., Ferrans, V. J., Irani, K., and Finkel, T. (1995) *Science 270*, 296−299.
3. Janes, S. M., Mu, D., Wemmer, D., Smith, A. J., Kaur, S., Maltby, D., Burlingame, A. L., and Klinman, J. P. (1990) *Science 248*, 981−987.
4. Matsuzaki, R., Fukui, T., Sato, H., Ozaki, Y., and Tanizawa, K. (1994) *FEBS Lett. 351*, 360−364.
5. Cai, D., and Klinman, J. P. (1994) *J. Biol. Chem. 269*, 32039−32042.
6. Klinman, J. P., and Mu, D. (1994) *Annu. Rev. Biochem. 63*, 299−344.
7. Janes, S. M. (1990) Ph.D. Dissertation, University of California, Berkeley, CA.
8. Medda, R., Padiglia, A., Pedersen, J. Z., and Floris, G. (1993) *Biochem. Biophys. Res. Commun. 196*, 1349−1355.
9. Frébort, I., Pec, P., Luhová, L., Matsushita, K., Toyama, H., and Adachi, O. (1994) *Eur. J. Biochem. 225*, 959−965.
10. Parsons, M. R., Convery, M. A., Wilmot, C. M., Yadav, K. D. S., Blakeley, V., Corner, A. S., Phillips, S. E. V., McPherson, M. J., and Knowles, P. F. (1995) *Structure 3*, 1171−1184.
11. Kumar, V., Dooley, D. M., Freeman, H. C., Guss, J. M., Harvey, I., McGuirl, M. A., Wilce, M. C., and Zubak, V. M. (1996) *Structure 4*, 943−955.
12. Li, R., Matthews, F. S., and Klinman, J. P. (1998) *Structure 6*, 293−307.
13. Wilmot, C. M., Murray, J. M., Alton, G., Parsons, M. R., Convery, M. A., Blakeley, V., Corner, A. S., Palcic, M. M., Knowles, P. F., McPherson, M. J., and Phillips, S. E. V. (1997) *Biochemistry 36*, 1608−1620.
14. Cai, D., and Klinman, J. P. (1994) *Biochemistry 33*, 7647−7653.
15. Ruggiero, C. E., Smith, J. A., Tanizawa, K., and Dooley, D. M. (1997) *Biochemistry 36*, 1953−1959.
16. Wilce, M. C. J., Dooley, D. M., Freeman, H. C., Guss, J. M., Matsunami, H., McIntire, W. S., Ruggiero, C. E., Tanizawa, K., and Yamaguchi, H. (1997) *Biochemistry 36*, 16116−16133.
17. Cai, D., Dove, J., Nakamura, N., Sanders-Loehr, J., and Klinman, J. P. (1997) *Biochemistry 36*, 11472−11478.
18. Neumann, R., Hevey, R., and Abeles, R. H. (1975) *J. Biol. Chem. 250*, 6362−6367.
19. Schowen, B. K., and Schowen, R. L. (1982) *Methods Enzymol. 87*, 551−606.
20. Loehr, T. M., and Sanders-Loehr, J. (1993) *Methods Enzymol. 226*, 431−470.
21. Robertson, J. G., Kumar, A., Mancewicz, J. A., and Villafranca, J. J. (1989) *J. Biol. Chem. 264*, 19916−19921.
22. Plastino, J. (1997) Ph.D. Dissertation, University of California, Berkeley, CA.
23. Mure, M., and Klinman, J. P. (1995) *J. Am. Chem. Soc. 117*, 8698−8706.
24. Brouwer, A. C., and Kirsch, J. F. (1982) *Biochemistry 21*, 1302−1307.
25. Glickman, M. H., and Klinman, J. P. (1995) *Biochemistry 34*, 14077−14092.
26. Nakamura, N., Moënne-Loccoz, P., Tanizawa, K., Mure, M., Suzuki, S., Klinman, J. P., and Sanders-Loehr, J. (1997) *Biochemistry 36*, 11479−11486.
27. Moënne-Loccoz, P., Nakamura, N., Steinebach, V., Duine, J. A., Mure, M., Klinman, J. P., and Sanders-Loehr, J. (1995) *Biochemistry 34*, 7020−7026.
28. Green, E. L., Nakamura, N., Tanizawa, K., Dooley, D. M., Klinman, J. P., and Sanders-Loehr, J. (1999) (in preparation).
29. Hevel, J. M., Mills, S. A., and Klinman, J. P. (1999) *Biochemistry 38*, 3683−3693.
30. Su, Q., and Klinman, J. P. (1998) *Biochemistry 37*, 12513−12525.
31. Gorren, A. C. F., Moënne-Loccoz, P., Backes, G., de Vries, S., Sanders-Loehr, J., and Duine, J. (1995) *Biochemistry 34*, 12926−12931.
32. Hartmann, C., and Klinman, J. P. (1987) *J. Biol. Chem. 262*, 962−965.
33. Hartmann, C., and Klinman, J. P. (1990) *FEBS Lett. 261*, 441−444.
34. Hartmann, C., Brzovic, P., and Klinman, J. P. (1993) *Biochemistry 32*, 2234−2241.
35. Mure, M., and Klinman, J. P. (1995) *J. Am. Chem. Soc. 117*, 8707−8718.
36. Mure, M., and Klinman, J. P. (1993) *J. Am. Chem. Soc. 115*, 7117−7127.
37. Schwartz, B., Green, E., Sanders-Loehr, J., and Klinman, J. P. (1998) *Biochemistry 37*, 16591.
38. Schanstra, J. P., and Janssen, D. B. (1996) *Biochemistry 35*, 5624−5632.
39. Zhou, J., and Adams, J. A. (1997) *Biochemistry 36*, 2977−2984.
40. Vignevich, V., Dooley, D. M., Guss, J. M., Harvey, I., McGuirl, M. A., and Freeman, H. C. (1993) *J. Mol. Biol. 229*, 243−245.

41. Brown, E. R. (1988) in *The Chemistry of Quinonoid Compounds* (Patai, S., and Rappoport, Z., Eds.) Vol. II, John Wiley and Sons, New York.
42. Dove, J., Schwartz, B., Williams, N. K., and Klinman, J. P. (1999) (in preparation).
43. Klinman, J. P. (1996) *Chem. Rev. 96*, 2541−2561.
44. Murray, J. M., Wilmot, C. M., Saysell, C. G., Jaeger, J., Knowles, P. F., Phillips, S. E. V., and McPherson, M. J. (1999) *Biochemistry 38*, 8217−8227.

BI9826660